



# Self-induced global rotation of chiral and other mechanical metamaterials

Krzysztof K. Dudek<sup>a,\*</sup>, Ruben Gatt<sup>b</sup>, Krzysztof W. Wojciechowski<sup>c</sup>, Joseph N. Grima<sup>b,d</sup>

<sup>a</sup> Institute of Physics, University of Zielona Gora, ul. Szafrana 4a, Zielona Gora 65-069, Poland

<sup>b</sup> Metamaterials Unit, Faculty of Science, University of Malta, Msida MSD 2080, Malta

<sup>c</sup> Institute of Molecular Physics, Polish Academy of Sciences, M. Smoluchowskiego 17, Poznan 60-179, Poland

<sup>d</sup> Department of Chemistry, Faculty of Science, University of Malta, Msida MSD 2080, Malta

## ARTICLE INFO

### Article history:

Received 23 February 2019

Revised 22 November 2019

Accepted 13 December 2019

Available online 19 December 2019

### Keywords:

Mechanical metamaterials

Composites

Global rotation

Molecular dynamics

Attitude control

## ABSTRACT

In this work, through the use of Molecular Dynamics simulations, we show the capability of different mechanical metamaterials to induce their own global rotational motion as a result of an internal deformation. We also show that one of the considered structures, i.e. the hexachiral system, may manifest a superior extent of the global rotation in comparison to other systems. In addition to that, we discuss that the self-induced global rotation can be observed for mechanical metamaterials with a discrete mass distribution which allows to prove that this phenomenon is not limited to macroscopic systems and applications involving the control of the rotational motion of objects such as satellites or wind turbines where the continuous mass distribution of structural elements is normally required. In fact, this study serves as a blueprint to show that a similar effect may also be expected for various systems at very different scales.

© 2019 Elsevier Ltd. All rights reserved.

## 1. Introduction

Mechanical metamaterials (Neville et al., 2016; Bertoldi et al., 2017; Mirzaali et al., 2018) are systems that can exhibit unusual mechanical properties as a result of their design rather than their chemical composition. Over the years, such systems have been thoroughly studied due to their capability to exhibit anomalous mechanical properties such as negative Poisson's ratio (auxetic behaviour) (Lakes, 1987; Wojciechowski, 1989; Evans et al., 1991; Milton, 1992; Sigmund, 1994; Grima and Evans, 2000; Hoover and Hoover, 2005; Alderson and Alderson, 2007; Shufrin et al., 2015; Lim, 2017; Jopek and Strek, 2018; Lim, 2019; Jiang et al., 2019), negative stiffness (Lakes, 2001; Wang and Lakes, 2004; Coulais et al., 2015; Yasuda and Yang, 2015; Hewage et al., 2016; Dudek et al., 2018a) negative compressibility (Lakes and Wojciechowski, 2008; Nicolaou and Motter, 2012; Cairns et al., 2013; Dudek et al., 2016; Qu et al., 2017) and negative thermal expansion (Mary et al., 1996; Sleight, 1998; Tucker et al., 2005; Wei et al., 2018) with all of these characteristics having a potential to impact our lives. More specifically, thanks to the efforts of scientists and the rapidly growing interest of different research communities in this field, a myriad of such systems have already been utilised in a variety

of applications ranging from biomedical (Gatt et al., 2014) to protective devices (Chan and Evans, 1998; Imbalzano et al., 2018; Francesconi et al., 2019) which we can benefit from on the daily basis. However, it is important to emphasise the fact that despite all of the studies conducted in the field of mechanical metamaterials there are still novel types of mechanical behaviour that remain unknown to the scientific community and may potentially lead to the application of these systems in new areas of the industry. It seems that one such concept corresponds to the recently reported potential of mechanical metamaterials to induce their own global rotational motion as a result of an internal deformation.

As reported in Dudek et al. (2017, 2018b), the self-induced global rotation of mechanical metamaterials is possible if the system is designed in an appropriate manner, i.e. if the mass within the system is distributed in a way leading to the generation of the non-zero net angular momentum associated with the motion of individual subunits constituting the structure during the deformation process of the entire system. This behaviour, that originates from the conservation of the angular momentum principle, was first studied (Dudek et al., 2017) through the use of a theoretical model where a particular example of a mechanical metamaterial in the form of the rotating square system was taken into consideration. In this work, it was shown that the extent of the global rotation can be controlled via the variation in the mass ratio of different groups of subunits. In the following work (Dudek et al., 2018b), the observation of the self-induced global rotation of a

\* corresponding author.

E-mail address: [k.dudek@if.uz.zgora.pl](mailto:k.dudek@if.uz.zgora.pl) (K.K. Dudek).

similar system was reported to be observed during an experimental study involving the use of a 3D-printed prototype. In the same work, through the use of a theoretical model, it was also analysed how the shape of subunits of different unimode metamaterials composed of rectangular structural motifs should be changed in order to maximise the extent of the global rotation of the entire system. All of these studies suggest that the self-induced global rotation can be observed for various types of mechanical metamaterials and that the extent of such motion can be controlled through the variation in different geometric parameters.

It is important to note that all of the structures which have been studied up to date from the point of view of their potential to induce their own global rotational motion as a result of an internal deformation were unimode rotating rigid unit systems composed of quadrilateral structural motifs. All of these systems consist of two groups of units rotating in opposite directions during the deformation process. This results in a situation where units rotating in opposite directions generate the opposite angular momentum meaning that the net angular momentum which is used to induce the global rotation of the entire system, in terms of magnitude, is equal to a difference of angular momenta corresponding to these two groups of elements. Obviously, these systems are not the most optimal structures from the point of view of the maximum extent of the global rotation as the two groups of units promote the opposite direction of the global rotation. As a result, for a non-zero global rotation to be even manifested, it is normally necessary to assign a different mass to the two groups of rigid units in such systems. One should expect that a much more suitable candidate to exhibit a self-induced global rotation to a significant extent would be systems where all of the subunits exhibit the same type of motion promoting a specific type of the global rotation. As the matter of fact, due to extensive studies related to mechanical properties of mechanical metamaterials such systems have already been discovered and are known as chiral systems (Spadoni et al., 2009; Alderson et al., 2010; Klepka et al., 2013; Frenzel et al., 2017; Mizzi et al., 2018; Fu et al., 2018; Fernandez-Corbaton et al., 2019).

In addition to the efficiency of specific mechanical metamaterials in terms of the extent of the global rotation, it is also worth to note that the systems investigated with regards to this phenomenon in the literature (Dudek et al., 2017; Dudek et al., 2018b) are composed of units with a continuous mass distribution that can be easily manufactured at the macroscale. Such systems can be used in a variety of applications such as satellites, spacecraft, telescopes employed in space or wind turbines where they can be used in order to induce and / or control the rotational motion of the system. However, this does not mean that the concept of the self-induced global rotation cannot be observed at much smaller scale. As the matter of fact, one should expect that the self-induced global rotation should be possible to be observed irrespective of the size of the system as long as such process would satisfy conservation laws. The difference between structures at the molecular / nano-scale and other systems is that instead of structural elements with a continuous mass distribution it is essential to consider discrete mass distribution in order to check the potential of such systems to induce their own global rotational motion. It should also be noted that in general, the use of a theoretical model to analyse the behaviour of the system subjected to a mechanical deformation could be very tedious in the case of more complex systems. Thus, it is important to consider the use of other methods such as computer simulations which could be applied to an arbitrary system irrespective of its design. One class of simulations which has already been proven to reliably portray the behaviour of mechanical metamaterials subjected to different types of the mechanical deformation are molecular dynamics (MD) simulations (Dudek et al., 2007; Baimova et al., 2014) where it is possible to analyse the evolution of a system in time.

In view of the above, in this work, computer simulations in a form of Molecular Dynamics simulations will be used in order to analyse the potential of different mechanical metamaterial systems to induce their own global rotational motion as a result of an internal deformation. More specifically, this approach will be used in order to verify the possibility of the observation of such effect for different rotating rigid unit systems with a discrete mass distribution which could serve as an indication of the potential of certain nano-scale and other systems to exhibit this characteristic. In addition to that, through the use of the same approach, the behaviour of a particular chiral system and other rotating rigid units structures will be analysed in an attempt of identifying mechanical metamaterials capable of exhibiting a superior extent of the self-induced global rotation which in turn could encourage researchers to pursue studies related to this phenomenon and perhaps lead to its implementation in the industry in the near future.

## 2. Concept

The basic concept of the self-induced global rotation of mechanical metamaterials relies on the conservation of angular momentum principle. As a mechanical metamaterial deforms due to a presence of internal forces, its structural elements move with respect to the centre of mass of the entire system. Such motion exhibited by each of the structural elements constituting the system can be accompanied by the generation of an angular momentum. It is important to note that for certain appropriately designed systems, the sum of angular momenta associated with all of the individual subunits of the system results in a non-zero net vector. This means, that if the structure is initially at rest, then the non-zero net angular momentum generated by structural elements must be compensated by the angular momentum associated with the global rotation of the entire system with respect to its centre of mass in order to conserve the total angular momentum. Thus, in general, mechanical metamaterials may induce their own global rotational motion without the application of any external forces to the system. This is particularly useful in the case of applications such as satellites and other objects employed in space where there is no possibility to apply the external force to the system to control its motion.

## 3. Model

### 3.1. Investigated systems

In this work, two types of rotating rigid unit systems, i.e. the rotating square system (Grima and Evans, 2000) and the triangle-based system (Dudek et al., 2016) composed of equilateral triangles (see Fig. 1(a-b)) as well as the hexachiral structure (Alderson et al., 2010) (see Fig. 1(c)) were studied in relation to their potential to exhibit a self-induced global rotation. It is worth to note that the triangle-based system considered in this work is different from the so-called rotating triangle system which term is often used in the case of the structure having six triangles constituting the structural unit (Grima and Evans, 2006). All of the systems investigated in this study are assumed to be composed of points having a non-zero mass that are arranged into specific two-dimensional geometries. To form structural elements, all of the points within each of the considered systems interact with each other by means of two-body as well as three-body bonded interactions (see section Interactions) as shown schematically in Fig. 1.

The first of the investigated structures, i.e. the rotating square system (see Fig. 1), is composed of three types of points having masses  $m_{L1}$ ,  $m_{H1}$  and  $m_1$ . Masses  $m_{L1}$  and  $m_{H1}$  are assigned to units that would rotate in opposite directions during the deformation process of the entire structure. As discussed in Dudek

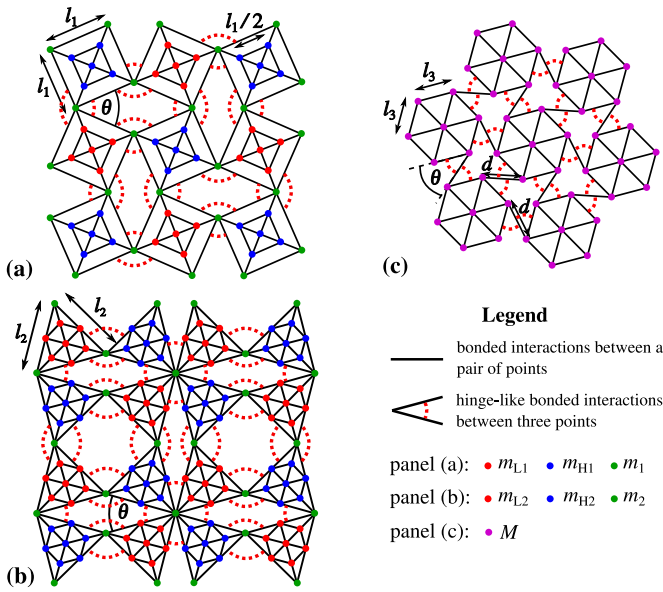


**Fig. 1.** Panels show all of the systems investigated in this work, i.e. (a) rotating square-system, (b) triangle-based system composed of equilateral triangles and (c) a hexachiral system. For each of the considered systems, all of the points (see the legend) interact with each other by means of two and three body bonded interactions governed by the appropriate harmonic potential. For the sake of clarity, three body bonded interactions between points forming the same structural unit are not indicated in this figure (see Appendix A).

et al. (2017, 2018b), this manner of a mass distribution allows to maximise the extent of the global rotation for the considered rotating rigid unit system. In addition to that, one should note that in the corners connecting neighbouring structural units there are point-like masses assigned that correspond to the value of  $m_1$ . In general, to ensure a large extent of the global rotation, masses constituting the rotating square system should satisfy the following condition  $m_{H1} > m_{L1}$ . Furthermore, in terms of the geometry, the system is composed of  $3 \times 3$  structural units having a side length of  $l_1$ . One may also note that within each of the square-like units there is a smaller unit having the same geometry that corresponds to a linear dimension  $l_1/2$ . It should be also noted that the angle between the neighbouring structural units is denoted as  $\theta$  with its value changing during the deformation process. The maximum range of values that this variable may assume due to geometric constraints is  $[0, \pi]$  rad.

The triangle-based system shown in Fig. 1(b) is composed of equilateral triangles having a linear dimension of  $l_2$  that have regular hexagons inscribed into them. Each of the vertices of such hexagons corresponds either to the mass denoted as  $m_{H2}$  or  $m_{L2}$  depending on the position of triangular units within the system. The angle between neighbouring units is denoted as  $\theta$  and it may assume any value from the interval  $[0, \pi/3]$  rad where its value changes during the deformation process. For this structure, similarly to what was the case for the rotating square system, points located at vertices of structural units have a different mass than other points and in this case such mass is denoted as  $m_2$ . It is important to note that as opposed to the rotating square system, this particular structure cannot be designed in a form of a lattice composed of  $N \times N$  structural units if  $N$  is an odd number. This stems from the fact that such design would result in one of the triangular units moving independently with respect to the rest of the system as it would be attached to the remaining part of the structure by means of only one vertex. In view of this, all of the examples of this system which are going to be considered in this work correspond to  $N \times N$  lattices with  $N$  being an even number.

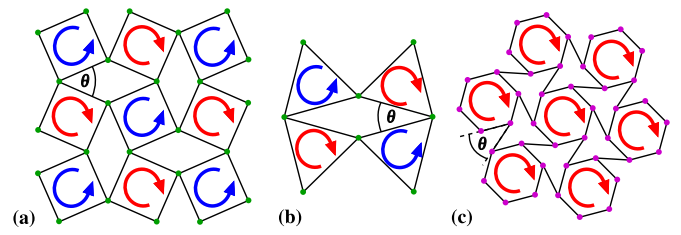


**Fig. 2.** Panels show the direction of rotation of individual units of the systems considered in this work upon being subjected to a deformation corresponding to a change in the value of  $\theta$ . For the sake of clarity, numerous details corresponding to the design of each of the systems that are shown in Fig. 1 are not presented.

As a result, the centre of mass of the entire structure is not a part of any of the structural units.

In addition to the rotating rigid unit systems described above, another structure which is investigated in this work is a hexachiral system composed of regular hexagon-shaped structural units having a linear dimension  $l_3$  (see Fig. 1(c)). The units constituting the system are connected to each other by means of rigid ligaments having a length of  $d$ . The angle between the ligament and the side of the hexagonal unit which the ligament is attached to is denoted as  $\theta$  and it may assume any value from the interval  $[0, \frac{4}{3}\pi]$  rad. It is important to note that as opposed to all of the formerly described structures, this system is composed of points having exactly the same mass that is denoted as  $M$ .

### 3.2. Deformation process

The deformation process for each of the considered systems corresponds to a change in angle  $\theta$  as described above. Due to the fact that points constituting each of the considered systems form rigid blocks having a particular geometry, the deformation of such structures can be analysed as a translational motion of structural units that is accompanied by their rotation. Furthermore, as discussed in the literature (Dudek et al., 2017; Dudek et al., 2018b), depending on the mass distribution and the direction of rotation of structural units, the entire system may exhibit a different type of a global rotation. In view of this, it is important to note that systems presented in Fig. 2(a-b) correspond to structures having their units rotating in opposite directions during the deformation process. On the other hand, in the case of the hexachiral system depicted in Fig. 2(c), all of the subunits rotate in the same direction which is very important from the point of view of the extent of the global rotation. More specifically, as opposed to systems shown on panels (a) and (b), in the case of the hexachiral system, the motion of all of the units contributes to a specific type of the global rotation exhibited by the entire structure. This means that one may expect that this particular structure may exhibit a larger extent of the global rotation than the other systems taken into consideration.

It should be also noted that the rotating square system and the triangle-based system have two sets of hinges within each of the apertures that promote the opposite direction of rotation of individual structural units. This allows to conveniently control the deformation of the system as an increase in the angle associated with one set of hinges leads to the opening of the structure while the increase in the angle corresponding to the other set of hinges results in the structure being closed. On the other hand, in the case of the hexachiral system, within each of the apertures there is only one type of hinges which stems from the fact that all of the units always rotate in the same direction.

### 3.3. Interactions

All of the points shown in Fig. 1 interact with other points by means of two-body bonded interactions that in the case of

this work are assumed to be governed by means of the harmonic potential  $V_2$  that can be described by means of the following equation:

$$V_2 = \frac{1}{2}k(l - l_0)^2 \quad (1)$$

where,  $l$  and  $l_0$  are the current distance and the equilibrium distance between a pair of points. The variable  $k$  stands for a stiffness constant and for all of the considered cases was set to be equal to  $15,000 \text{ Jm}^{-2}$ . This means that such bonds were made to be sufficiently rigid in order to ensure that distances between points from the same structural units would remain approximately constant throughout the entire deformation process.

$$V_{3,int} = \frac{1}{2}K_{int}(\alpha_i - \alpha_{i,0})^2 \quad \text{and} \quad V_{3,ext} = \frac{1}{2}K_{ext}(\theta - \theta_0)^2 \quad (2)$$

In addition to two-body bonded interactions, points constituting each of the considered systems are also assumed to interact with each other by means of two types of three-body bonded interactions with both of these interactions being governed by the harmonic potential for the rotational motion. More specifically, sets of three points that are located within the same structural unit are assumed to interact with each other by means of the harmonic potential  $V_{3,int}$  (see Eq. (2)) which is meant primarily to ensure the rigidity of structural units should the two-body interactions prove to be insufficient. Angle  $\alpha_i$ , used in the above definition of this potential, corresponds to the angle between two vectors formed upon connecting a given set of three interacting points. The reason why there is a subscript  $i$  in the definition of the angle  $\alpha_i$  is the fact that as shown in Appendix A, such angle may assume very different values depending on the position of a given set of three interacting points within the structural unit. Furthermore, the variable  $\alpha_{0,i}$  stands for the equilibrium angle associated with the configuration where there are not any forces acting on points associated with three-body bonded interactions corresponding to the angle  $\alpha_i$ . In this work, for all of the considered cases, different values of  $\alpha_{0,i}$  correspond to the shape of structural units that is portrayed in Fig. 1. It should be also noted that the way how three-body bonded interactions are defined within each of the structural units is shown in more detail in Appendix A.

Three-body bonded interactions that are shown in Fig. 1 have a different purpose than three-body bonded interactions describing the behaviour of points within the same structural unit. More specifically, these interactions, that are governed by means of the potential  $V_{3,ext}$ , are meant solely to induce the deformation of the structure which process corresponds to the change in the value of  $\theta$  (see Fig. 1). In this case, whenever the angle  $\theta$  assumes the value of  $\theta_0$  for a given group of three points, then there are not any forces acting on these points due to this particular potential. It should also be noted that the value of the constant  $K_{ext}$  that is used to define this potential in Eq. (2), is significantly smaller than  $K_{int}$  which stems from a different purpose of potentials  $V_{3,int}$  and  $V_{3,ext}$ . More specifically, for all of the examples considered in this work  $K_{int} = 1 \text{ J rad}^{-2}$  while  $K_{ext} = 10^{-4} \text{ J rad}^{-2}$ .

It is worth to keep in mind that the deformation of each of the considered systems corresponds to the change in the shape of an aperture between the structural elements which change is related to the variation in the value of  $\theta$ . Such behaviour originates from the hinging motion exhibited by adjacent structural elements. The hinging mechanism can be described by two ligaments sharing the same vertex which means that in fact, the hinging motion is defined by different sets of three points which are graphically shown in Fig. 1. The behaviour exhibited by each set of such points is described by three-body bonded interaction where in the case of this work it is assumed that such motion is governed by means of the harmonic potential (see Eq. (2)). As a result, there is a force acting on each of the points being a part of the hinge governed

by the harmonic potential, where such force can be determined in a standard manner as a gradient of the aforementioned harmonic potential.

It is important to note that three-body bonded interactions allow to analyse the maximum possible extent of the mechanical deformation permissible by each of the geometries. This in turn would not be possible should one decide to induce the deformation of the system by a change in distance between some two specific points selected within the system. This stems from the fact that in such the case, the maximum deformation could be only induced as a result of the transition of the system from the fully open to the fully closed structure or vice versa. However, it is clear that for structures such as the rotating square system or the hexachiral system such transition would cover only a certain part of the geometrically permissible deformation. Thus, the maximum extent of the global rotation for a given system cannot be determined which is one of the objectives of this work.

### 3.4. Simulations

The results discussed in this work were generated through the use of Molecular Dynamics simulations making use of the fourth-order Runge-Kutta algorithm (Burden and Faires, 1985) with a constant time-step  $\Delta t = 10^{-5} \text{ s}$ . For each of the considered systems, the structure that was initially at rest was released at the time  $t = 0 \text{ s}$  which action was followed by the deformation of the system that was induced by appropriately defined bonded interactions. In the case of all of the considered simulations, the behaviour of the system during such deformation process was analysed up to the moment of the collision between structural units constituting the system.

In the case of all of the systems considered in this work, the extent of the self-induced global rotation is quantified by means of the angle  $\Delta\theta_1$ . This variable can be defined through the use of an auxiliary vector connecting the centre of mass of the entire system and the centre of one of the neighbouring structural units. This stems from the fact that as the system is being deformed, the orientation of such auxiliary vector changes as the position of the centre of the selected structural unit is being changed in time. Thus, in the case of a system where in accordance to the conservation principles one should not expect the occurrence of the global rotation, the orientation of the aforementioned vector should not change irrespective of the extent of the mechanical deformation. As a result, one can calculate the extent of the self-induced global rotation of the entire system as an angle between the considered auxiliary vector defined in the case of the system assuming its initial and final configuration during the deformation process respectively. It is also important to remember that the global rotation always occurs with respect to the centre of mass of the entire system.

Simulations corresponding to different structures considered in this work were conducted for different sets of initial parameters. More specifically, for the rotating square system shown in Fig. 1(a):  $l_1 = 2 \text{ cm}$ ,  $m_{H1} = \{6.44, 8.28, 9.16, 9.66, 10.00\} \text{ g}$ ,  $m_{L1} = \{6.44, 4.14, 3.05, 2.42, 2.00\} \text{ g}$ ,  $m_1 = 1.8 \text{ g}$ ,  $\theta(t = 0) = 180^\circ$ , for the triangle-based system shown in Fig. 1(b):  $l_2 = 2 \text{ cm}$ ,  $m_{H2} = \{6.0, 8.0, 9.0, 9.6, 10.0\} \text{ g}$ ,  $m_{L2} = \{6.0, 4.0, 3.0, 2.4, 2.0\} \text{ g}$ ,  $m_2 = 1.8 \text{ g}$ ,  $\theta(t = 0) = 60^\circ$  and for the hexachiral system shown in Fig. 1(c):  $M = 5 \text{ g}$ ,  $l_3 = 2 \text{ cm}$ ,  $d = \{2, 10, 20\} \text{ cm}$ ,  $\theta(t = 0) = 0^\circ$ .

## 4. Results and discussion

Based on results shown in Fig. 3, one may note that all of the analysed systems are capable of exhibiting a self-induced global rotation with the extent of such rotation depending on the type of the structure. It may be also noted that for all of the systems,



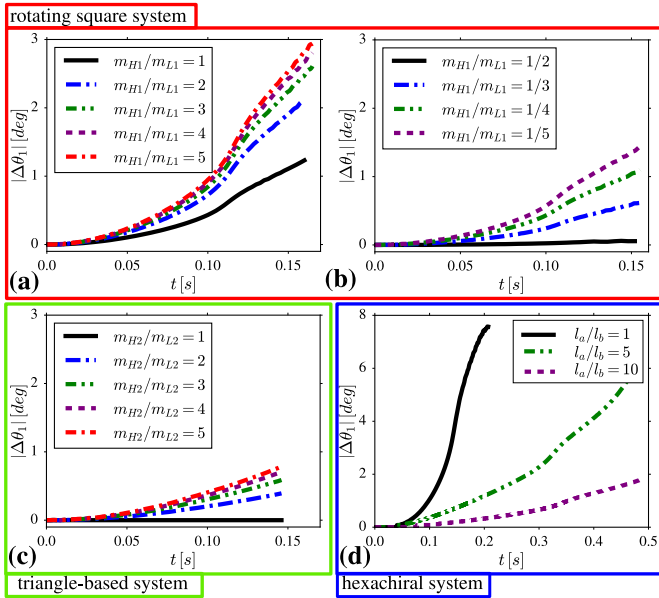


**Fig. 3.** Graphs show the variation in the extent of the global rotation observed in time for different systems that are analysed in this work. It is important to highlight the fact that in all of the considered cases, graphs show the behaviour of investigated systems from the moment when they were released up to the moment of the collision between their structural elements.

the change in the mass distribution and / or geometric parameters leads to a different global rotation. This means that irrespective of the type of an investigated system, the extent of the global rotation can be controlled through the variation in the mass distribution and geometry of the structure. This particular behaviour can be analysed quantitatively for each of the considered systems. More specifically, as shown in Fig. 3(a), in the case of the rotating square system composed of 5 relatively heavy and 4 relatively light structural units, one may maximise the extent of the global rotation manifested by the system upon increasing the ratio of masses corresponding to heavy and light units rotating in opposite directions ( $m_{H1}/m_{L1}$ ). This stems from the fact that such procedure allows to increase the net torque generated by all of the structural units during the deformation process. It should be also noted that upon increasing the value of the mass ratio for the system having a constant mass, the improvement in the extent of its global rotation becomes increasingly smaller. This in turn indicates that in reality there is no need to construct the system with extreme values of the  $m_{H1}/m_{L1}$  parameter in order to observe the extent of the global rotation that is close to its maximum value.

In addition to behaviour of the rotating square system composed of 5 relatively heavy and 4 relatively light structural units, one may also analyse the behaviour of the system where the four units rotating in a specific direction would be heavier than the remaining five structural units. As shown in Fig. 3(b), such situation leads to a significantly reduced extent of the global rotation than was the case for the system with 5 heavy structural units. This stems from the fact that in this scenario, there is a larger number of light units that promote an opposite direction of the global rotation than heavier units and as a result the net torque generated by all of the units is relatively small.

According to Fig. 3(c), similarly to the rotating square structure, the triangle-based system analysed in this work is capable of inducing its own global rotational motion as a result of an internal deformation. However, in this case, the extent of the global rotation is equal to zero should one assume that masses of points located on triangular units rotating in the opposite directions during the deformation process are the same, i.e.  $m_{H2}/m_{L2} = 1$ . This

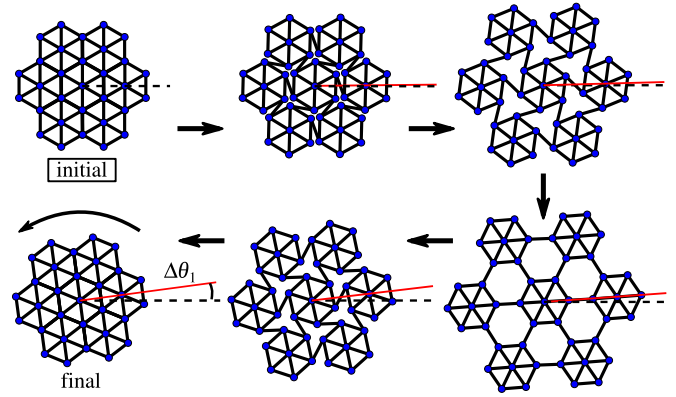


**Fig. 4.** The evolution of the hexachiral system in the case when  $l_3 = d$ . The extent of the global rotation  $\Delta\theta_1$  is represented by an angle between an auxiliary dashed black line that passes through the centre of the entire system and the centre of one of the neighbouring units at the moment when the structure is at its initial configuration and the red line that passes through the same two points in the case of the final configuration assumed by the system. Due to initial conditions, the presented system exhibits the global rotation in the anticlockwise direction as a result of an internal deformation which rotation is indicated by means of a black arrow in the case of the final configuration assumed by the system. (For interpretation of the references to colour in this figure legend, the reader is referred to the web version of this article.)

particular result originates from the fact that for this structure, the number of units rotating in the opposite directions is exactly the same. Furthermore, one may note that upon changing the mass ratio  $m_{H2}/m_{L2}$ , the extent of the global rotation starts assuming non-zero values. More specifically, the larger the difference between  $m_{H2}$  and  $m_{L2}$ , the larger the extent of the global rotation. At this point, it is also important to emphasize the fact that the extent of the global rotation associated with the triangle-based system is significantly smaller than is the case for the rotating square system. One of the reasons leading to this situation is the fact that the rotating square system can be arranged in the configuration where there is a bigger number of structural units rotating in a specific direction than in the opposite direction. However, it seems that an even more important reason is the fact that due to geometric constraints, in the case of the triangle-based system angle  $\theta$  may change only by  $60^\circ$  during the deformation process where in the case of the rotating square system the change in  $\theta$  may reach as much as  $180^\circ$ . Thus, rotating square units can rotate to a much larger extent during the deformation process which motion contributes to the global rotation exhibited by the structure.

The last of the investigated systems is the hexachiral structure depicted in Fig. 1(c). As shown in Fig. 3(d), this particular system exhibits a very large extent of the global rotation in comparison to all of the formerly studied mechanical metamaterials. As already mentioned in the section Deformation process, this particular result originates from a way how chiral systems deform. More specifically, during the deformation process all of the structural units exhibit the same type of motion that promotes a specific type of the global rotation. On the other hand, in the case of the formerly analysed rotating rigid unit systems, there were always two groups of structural units that were promoting an opposite direction of the global rotation and hence making the entire process inefficient. The extent of the global rotation observed for the best analysed scenario of the hexachiral system with  $l_3 = d$ , is shown graphically in Fig. 4.

It is also interesting to analyse the effect that the variation in the geometry of the hexachiral system has on the extent of its global rotation. It seems that the most suitable geometric parameter that can be used in order to conduct such analysis is the length of ligaments  $l$ . Based on Fig. 3(d), one may note that the variation

in the value of  $l$  has indeed a very large impact on the extent of the global rotation exhibited by the deforming hexachiral structure. More specifically, the largest extent of the global rotation can be observed for relatively short ligaments connecting structural units which corresponds to the situation where the entire system has a relatively small moment of inertia. Furthermore, for significantly larger values of  $l$ , the extent of the global rotation is clearly reduced as the moment of inertia associated with the rotation of the entire system with respect to its centre of mass gets increased. At this point, it is also worth to note that a similar analysis to the one provided above can be conducted based on the results showing the variation in the extent of the global rotation plotted against the change in the geometric parameter which is indicative of the stage of the internal deformation, i.e. angle  $\theta$ . As shown in Appendix B (see Fig. B1), results corresponding to the change in the angle  $\theta$  lead to the same conclusions as the results associated with the variation in the extent of the global rotation plotted against time.

At this point, one may also note that both the rotating square system and the triangle-based system are unimode structures, hence due to the constraints imposed by the hinges, all of the units are forced to rotate with the same angular velocity (in terms of magnitude). However, the hexachiral system is more prone to the occurrence of some imperfections in the deformation mechanism even if they were to be relatively small. For example the central hexagon may rotate with a slightly different angular velocity than the hexagons forming the outer layer of the structure as they have a different number of ligaments connecting them with their neighbours. Nevertheless, irrespective of some potential small imperfections, all of the units are always forced to rotate in the same direction, hence the direction nor the magnitude of the self-induced global rotation are not expected to be significantly affected by such effects. To further minimise the presence of potential imperfections one can fine-tune the rigidity of ligaments connecting the adjacent structural units.

All of this is very important as in this work, it is shown that several very different mechanical metamaterials are capable of inducing their own global rotational motion as a result of an internal deformation. In particular, upon taking the hexachiral structure as an example, it is shown that chiral systems can manifest a superior extent of the considered phenomenon in comparison to common examples of rotating rigid unit systems. It is also interesting to note that in the case of all of the considered systems, the global rotation was observed for structures with a discrete mass distribution. This in turn indicates that the concept of the self-induced global rotation of mechanical metamaterials does not have to be limited to macroscopic systems having a continuous mass distribution that can be utilised in the case of applications involving the control of the rotational motion of satellites and telescopes employed in space or wind turbines. Instead, this result serves as a blueprint to show that the effect of the self-induced global rotation should be possible to be observed in the case of nano-scale systems that similarly to models discussed in this work have a discrete mass distribution. As the matter of fact, in the literature there are already examples of experimental studies related to systems at the nano-scale which closely resemble those investigated in this work and are characterised by very similar mechanical properties (Suzuki et al., 2016). It should be also emphasised that the concept of the self-induced global rotation is not limited to structures discussed in this work. In fact, this effect should be expected to be observed for any system where as a result of an internal deformation a non-zero net angular momentum is generated. It should be also noted that in order for the discussed phenomenon to be manifested, the structural elements of the system must be able to move in order to generate the non-zero net angular which process is limited by geometric constraints of a given system. Thus the global rotation can be exhibited only until the moment when the

structure assumes a locked configuration. However, in general the global rotation can be manifested for a very long time should the hinges connecting structural elements of the system be designed in the appropriate manner. A very good example of such solution incorporating the use of electromagnetic hinges is discussed in the recent work related to the concept of the self-induced global rotation of mechanical metamaterials (Dudek et al., 2018b).

## 5. Conclusion

In this work, through the use of Molecular Dynamics simulations, it was shown that different mechanical metamaterials with a discrete mass distribution can induce their own global rotational motion as a result of an internal deformation. It was also shown that one of the investigated systems, i.e. the hexachiral structure, can manifest a superior extent of the global rotation in comparison to other mechanical metamaterials that were studied up to date from the point of view of their potential to exhibit this phenomenon. Furthermore, it was shown that for all of the considered mechanical metamaterials, the extent of the global rotation can be controlled via the variation in the mass distribution and geometric parameters of the system. Finally, it was discussed that the fact that in this work the self-induced global rotation could be observed in the case of systems with a discrete mass distribution could serve as a blueprint to show that this phenomenon could be manifested by systems at very different scales including the nano-scale. This in turn may encourage researchers to implement this concept in the case of various structures that can undergo a similar deformation process to systems investigated in this work.

## Declaration of Competing Interest

The authors declare that they have no known competing financial interests or personal relationships that could have appeared to influence the work reported in this paper.

## CRediT authorship contribution statement

**Krzysztof K. Dudek:** Conceptualization, Methodology, Investigation, Writing - original draft. **Ruben Gatt:** Investigation, Writing - original draft, Supervision. **Krzysztof W. Wojciechowski:** Supervision. **Joseph N. Grima:** Validation, Supervision.

## Acknowledgments

K.K.D. is supported by the Foundation for Polish Science (FNP). K.K.D. acknowledges the financial support from the program of the Polish Minister of Science and Higher Education under the name Regional Initiative of Excellence in 2019 - 2022, project no. 003/RID/2018/19, funding amount 11 936 596.10 PLN. We would also want to sincerely thank Prof. Mirosław Dudek from the University of Zielona Góra for his help and useful remarks that he had offered us during our work on this project.

## Appendix A. Three body interactions within structural units

The sole purpose of three-body interactions corresponding to sets of three points located within the same structural unit is to ensure the rigidity of structural units should two-body interactions prove to be insufficient. For the sake of clarity, these interactions were not marked in the case of Fig. 1. In view of this, in order to better explain how such interactions were defined, three-body bonded interactions corresponding to structural units of each of the systems considered in this work are shown in Fig. A.1. In this case, each set of three points connected by means of an auxiliary green dashed arc corresponds to a specific value of  $\alpha_i$  and  $\alpha_{i,0}$  in Eq. (2).

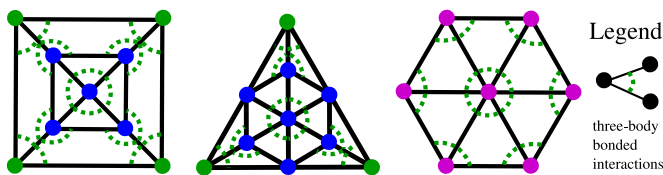


**Fig. A1.** Diagrams showing the way how three-body interactions were defined within each type of the structural units that was considered in this work.

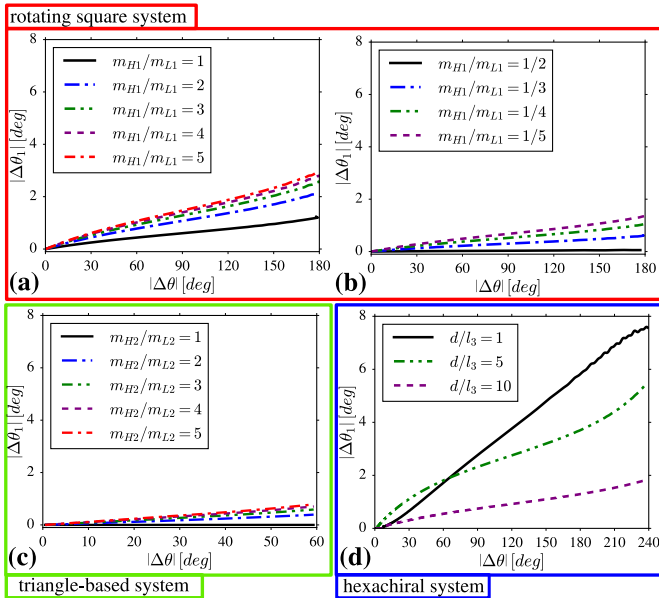


**Fig. B1.** Variation in the extent of the global rotation expressed in terms of the change in the value of the integral angle  $\theta$ .

## Appendix B. Extent of the global rotation expressed in terms of the variation in $\theta$

In addition to the analysis of the results corresponding to the variation in the extent of the global rotation plotted against time (see Fig. 3), one can also show how the change in the extent of the global rotation depends on the value of the internal angle  $\theta$  which for all of the considered structures defines the extent of the mechanical deformation. As shown in Fig. B.1, the generated results show the same trends as was the case for plots portraying the dependence of the extent of the global rotation on time. In view of this, similarly to the analysis conducted in the Results and Discussion section, it is possible to note that hexachiral system has the potential to exhibit the largest extent of the self-induced global rotation in comparison to other structures taken into consideration.

## References

Alderson, A., Alderson, K.L., 2007. Auxetic materials. *Proc. Inst. Mech. Eng. G* 221, 565–575.  
 Alderson, A., Alderson, K.L., Attard, D., Evans, K.E., Gatt, R., Grima, J.N., Miller, W., Ravirala, N., Smith, C.W., Zied, Z., 2010. Elastic constants of 3-, 4- and 6-connected chiral and anti-chiral honeycombs subject to uniaxial in-plane loading. *Compos. Sci. Technol.* 70, 1042–1048.  
 Baimova, J.A., Liu, B., Dmitriev, S.V., Zhou, K., 2014. Mechanical properties and structures of bulk nanomaterials based on carbon nanopolymorphs. *Phys. Status Solidi RRL* 8, 336–340.  
 Bertoldi, K., Vitelli, V., Christensen, J., van Hecke, M., 2017. Flexible mechanical metamaterials. *Nat. Rev. Mater.* 2, 17066.  
 Burden, R.L., Faires, J.D., 1985. *Numerical Analysis*. PWS.  
 Cairns, A.B., Catafesta, J., Levelut, C., Rouquette, J., van der Lee, A., Peters, L., Thompson, A.L., Dmitriev, V., Haines, J., Goodwin, A.L., 2013. Giant negative linear compressibility in zinc dicyanoaurate. *Nat. Mater.* 12, 212–216.  
 Chan, N., Evans, K.E., 1998. Indentation resilience of conventional and auxetic foams. *J. Cell. Plast.* 34, 231–260.

Coulais, C., Overvelde, J.T.B., Lubbers, L.A., Bertoldi, K., van Hecke, M., 2015. Discontinuous buckling of wide beams and metabeams. *Phys. Rev. Lett.* 115, 044301.  
 Dudek, K.K., Attard, D., Caruana-Gauci, R., Wojciechowski, K.W., Grima, J.N., 2016. Unimode metamaterials exhibiting negative linear compressibility and negative thermal expansion. *Smart Mater. Struct.* 25, 025009.  
 Dudek, K.K., Gatt, R., Dudek, M.R., Grima, J.N., 2018. Negative and positive stiffness in auxetic magneto-mechanical metamaterials. *Proc. R. Soc. A* 474, 20180003.  
 Dudek, K.K., Gatt, R., Mizzi, L., Dudek, M.R., Attard, D., Grima, J.N., 2017. Global rotation of mechanical metamaterials induced by their internal deformation. *AIP Adv.* 7, 095121.  
 Dudek, K.K., Wojciechowski, K.W., Dudek, M.R., Gatt, R., Mizzi, L., Grima, J.N., 2018. Potential of mechanical metamaterials to induce their own global rotational motion. *Smart Mater. Struct.* 27, 055007.  
 Dudek, M.R., Grabiec, B., Wojciechowski, K.W., 2007. Molecular dynamics simulations of auxetic ferrogel. *Rev. Adv. Mater. Sci.* 14, 167–173.  
 Evans, K.E., Nkansah, M.A., Hutchinson, I.J., Rogers, S.C., 1991. Molecular network design. *Nature* 353, 124.  
 Fernandez-Corbaton, I., Rockstuhl, C., Ziemke, P., Gumbsch, P., Albiez, A., Schwaiger, R., Frenzel, T., Kadic, M., Wegener, M., 2019. New twists of 3d chiral metamaterials. *Adv. Mater.* 31, 1807742.  
 Francesconi, L., Baldi, A., Liang, X., Aymerich, F., Taylor, M., 2019. Variable poisson's ratio materials for globally stable static and dynamic compression resistance. *Extreme Mech. Lett.* 26, 1–7.  
 Frenzel, T., Kadic, M., Wegener, M., 2017. Three-dimensional mechanical metamaterials with a twist. *Science* 358, 1072–1074.  
 Fu, M., Liu, F., Hu, L., 2018. A novel category of 3d chiral material with negative poisson's ratio. *Compos. Sci. Technol.* 160, 111–118.  
 Gatt, R., Caruana-Gauci, R., Attard, D., Casha, A.R., Wolak, W., Dudek, K., Mizzi, L., Grima, J.N., 2014. On the properties of real finite-sized planar and tubular stent-like auxetic structures. *Phys. Status Solidi B* 251, 321–327.  
 Grima, J.N., Evans, K.E., 2000. Auxetic behavior from rotating squares. *J. Mater. Sci. Lett.* 19, 1563–1565.  
 Grima, J.N., Evans, K.E., 2006. Auxetic behavior from rotating triangles. *J. Mater. Sci.* 41, 3193–3196.  
 Hewage, T.A.M., Alderson, K.L., Alderson, A., Scarpa, F., 2016. Double-negative mechanical metamaterials displaying simultaneous negative stiffness and negative poisson's ratio properties. *Adv. Mater.* 28, 10323.  
 Hoover, W.G., Hoover, C.G., 2005. Searching for auxetics with DYN3D and paradyn. *Phys. Status Solidi B* 242, 585–594.  
 Imbalzano, G., Linforth, S., Ngo, T.D., Lee, P.V.S., Tran, P., 2018. Blast resistance of auxetic and honeycomb sandwich panels: comparisons and parametric designs. *Compos. Struct.* 18, 242–261.  
 Jiang, Y., Rudra, B., Shim, J., Li, Y., 2019. Limiting strain for auxeticity under large compressive deformation: chiral vs. re-entrant cellular solids. *Int. J. Solids Struct.* 162, 87–95.  
 Jopek, H., Strek, T., 2018. Thermoauxetic behavior of composite structures. *Materials* 11, 294.  
 Klepka, A., Staszewski, W.J., di Maio, D., Scarpa, F., 2013. Impact damage detection in composite chiral sandwich panels using nonlinear vibro-acoustic modulations. *Smart Mater. Struct.* 22, 084011.  
 Lakes, R., 1987. Foam structures with a negative poisson's ratio. *Science* 235, 1038–1040.  
 Lakes, R., Wojciechowski, K.W., 2008. Negative compressibility, negative poisson's ratio, and stability. *Phys. Status Solidi B* 245, 545–551.  
 Lakes, R.S., 2001. Extreme damping in compliant composites with a negative-stiffness phase. *Philos. Mag. Lett.* 81, 95–100.  
 Lim, T.-C., 2017. Analogies across auxetic models based on deformation mechanism. *Phys. Status Solidi RRL* 11, 1600440.  
 Lim, T.-C., 2019. An anisotropic auxetic 2d metamaterial based on sliding microstructural mechanism. *Materials* 12, 429.  
 Mary, T.A., Evans, J.S.O., Vogt, T., Sleight, A.W., 1996. Negative thermal expansion from 0.3 to 1050 kelvin in zrwo<sub>2</sub>. *Science* 272, 90–92.  
 Milton, G.W., 1992. Composite materials with poisson's ratios close to 1. *J. Mech. Phys. Solids* 40, 1105–1137.  
 Mirzaali, M.J., Caracciolo, A., Pahlavani, H., Janbaz, S., Vergani, L., Zadpoor, A.A., 2018. Multi-material 3D printed mechanical metamaterials: rational design of elastic properties through spatial distribution of hard and soft phases. *Appl. Phys. Lett.* 113, 241903.  
 Mizzi, L., Attard, D., Gatt, R., Farrugia, P.-S., Grima, J.N., 2018. An analytical and finite element study on the mechanical properties of irregular hexachiral honeycombs. *Smart Mater. Struct.* 27, 105016.  
 Neville, R.M., Scarpa, F., Pirrera, A., 2016. Shape morphing kirigami mechanical metamaterials. *Sci. Rep.* 6, 31067.  
 Nicolaou, Z.G., Motter, A.E., 2012. Mechanical metamaterials with negative compressibility transitions. *Nat. Mater.* 11, 608–613.  
 Qu, J., Kadic, M., Wegener, M., 2017. Poroelectric metamaterials with negative effective static compressibility. *Appl. Phys. Lett.* 110, 171901.  
 Shufrin, I., Pasternak, E., Dyskin, A.V., 2015. Negative poisson's ratio in hollow sphere materials. *Int. J. Solids Struct.* 54, 192–214.  
 Sigmund, O., 1994. Materials with prescribed constitutive parameters: an inverse homogenization problem. *Int. J. Solids Struct.* 31, 2313–2329.  
 Sleight, A.W., 1998. Negative thermal expansion materials. *Curr. Opin. Solid State Mater. Sci.* 3, 128–131.  
 Spadoni, A., Ruzzene, M., Gonella, S., Scarpa, F., 2009. Phononic properties of hexagonal chiral lattices. *Wave Motion* 46, 435–450.

- Suzuki, Y., Cardone, G., Restrepo, D., Zavattieri, P.D., Baker, T.S., Akif Tezcan, F., 2016. Self-assembly of coherently dynamic, auxetic, two-dimensional protein crystals. *Nature* 533, 369–373.
- Tucker, M.G., Goodwin, A.L., Dove, M.T., Keen, D.A., Wells, S.A., Evans, J.S.O., 2005. Negative thermal expansion in ZrW<sub>2</sub>O<sub>8</sub> mechanisms, rigid unit modes, and neutron total scattering. *Phys. Rev. Lett.* 95, 255501.
- Wang, Y.C., Lakes, R.S., 2004. Extreme stiffness systems due to negative stiffness elements. *Am. J. Phys.* 72, 40–50.
- Wei, K., Peng, Y., Qu, Z., Pei, Y., Fang, D., 2018. A cellular metastructure incorporating coupled negative thermal expansion and negative poisson's ratio. *Int. J. Solids Struct.* 150, 255–267.
- Wojciechowski, K., 1989. Two-dimensional isotropic system with a negative poisson ratio. *Phys. Lett. A* 137, 60–64.
- Yasuda, H., Yang, J., 2015. Reentrant origami-based metamaterials with negative poisson's ratio and bistability. *Phys. Rev. Lett.* 114, 185502.